EFFECTS OF REDUCTION AND SIZE OF GRAPHENE ON MECHANICAL AND ELECTRICAL PROPERTIES OF GRAPHENE OXIDE PAPERS

Xiuyi Lin, Qingbin Zheng, Nariman Yousefi, Kan Kan Yeung, Xi Shen, Jang-Kyo Kim*

Department of Mechanical Engineering, The Hong Kong University of Science and Technology, Clear Water Bay, Kowloon, Hong Kong
**e-mail address of the corresponding author: mejkkim@ust.hk*

Keywords: Graphene oxide, graphene oxide paper, mechanical property.

Abstract
The effects of graphene oxide (GO) size and reduction method on mechanical property and electrical conductivity of GO papers are studied. GO sheets are prepared using the modified Hummers method and GO papers are fabricated through vacuum filtration of GO aqueous dispersions. To study the size effect, the as-prepared GO dispersion is sorted into four different groups with uniform sizes after repeated centrifugation and collection of supernatant. It is found that the Young's modulus, tensile strength and electrical conductivity increase consistently with increasing the GO size. Three methods, including hydrazine reduction, hydrogen iodide reduction and thermal treatment, are employed to reduce the GO sheets. The highest electrical conductivity of 139,000 S/m is obtained after thermal reduction. The mechanisms responsible for these observations are discussed based on the elemental, structural and morphological analyses of GO and reduced GO sheets.

1 Introduction
Graphene oxide (GO) consists of a single or a few layer graphene sheets with oxygenated functional groups attached on their basal planes and edges. GO paper is a free-standing paper-like material that is fabricated by stacking GO sheets via flow-directed assembly of aqueous GO dispersion. This new material outperforms many other paper-like materials in mechanical properties [1]. The tensile modulus and strength of GO paper are found to be comparable to those of flexible graphite foils and pristine carbon nanotube bucky papers prepared by filtration [2]. The combination of exceptional mechanical properties [3], thermal stability [4], high electrical conductivity [5] and biocompatibility [6] make GO papers a promising candidate for many applications, ranging from free-standing, flexible electrodes for Li ion batteries [7] to biomedical implants [8].

The lateral dimensions of precursor GO sheets are considered playing an important role in controlling properties and applications of GO papers. For example, large GO sheets are ideally suited in a number of applications, e.g. forming three-dimensional graphene-based networks [9], developing an aligned structure in polymer-based composites [10] and producing conductive thin films for optoelectronic devices [11]. Larger GO sheets can give rise to a higher electrical conductivity due to lower inter-sheet contact resistance than in small GO [12]. The thermal conductivity of GO papers was also a strong function of GO sheet size

[13]. Obviously, a more systematic study is necessary to establish the GO size-property relationship and understand the mechanisms responsible for its effects. It is equally important to synthesize GO with controlled sizes for desired applications. Several studies have appeared in the literature, which proposed methods to control the GO size in aqueous dispersion: namely i) an electrochemical technique by controlling the applied voltage, electrical current and reduction time [14]; ii) chemical exfoliation by controlling the oxidation and exfoliation process where the GO size decreased with oxidation time [15]; iii) size reduction due to energy generated by fluid motion or sonication causing tensile stresses to build up in the sheets [16]; and iv) adjusting the pH value of GO dispersion [17]. In this study, a simple method based on repeated centrifugation and collection of supernatant is proposed to sort as-produced GO sheets into four different size groups.

Another important factor that affects the electrical conductivity of GO papers is the degree of reduction. GO sheets consist of both sp^2 and sp^3 carbon, and the presence of oxygen-containing functionalities disturb the sp^2 bond, making GO an insulator. The reduced graphene oxide (rGO) contains a much lower oxygen concentration and becomes electrically conductive depending on the degree of reduction. Therefore, proper selection of reduction processes is essential to restoring the inherently high electrical conductivity of graphene.

2 Experimental

2.1 Synthesis of GO and GO papers

GO was synthesized based on the modified Hummers method using natural graphite flakes (Asbury Graphite Mills), and the procedure used to prepare GO is described elsewhere [18, 19]. The as-produced GO dispersion contained 1.0 mg/ml of mostly mono-layer GO sheets with largely different sizes in water. The GO was sorted into four groups with uniform sizes through three-step centrifugation on a table-top centrifuge (SIGMA 2-16P), as shown in Figure 1. The unsorted GO dispersion was initially centrifuged at 8000 rpm for 40 min, dividing into supernatant and precipitate. The precipitate was collected for the second round of centrifugation, while the supernatant was designated as small GO (S-GO). The collected precipitate was dispersed in water and centrifuged at increasingly reduced speeds for another two runs to collect large GO (L-GO), very large GO (VL-GO) and ultra large GO (UL-GO) [12]. The GO paper was prepared by filtration of GO dispersion before or after chemical reduction through a membrane filter (Anodisc with 47 mm in diameter and 0.2 mm pore size, supplied by Whatman) with the aid of vacuum. After filtration, the paper was peeled off from the filter membrane and dried in an oven at 60 ℃ overnight.

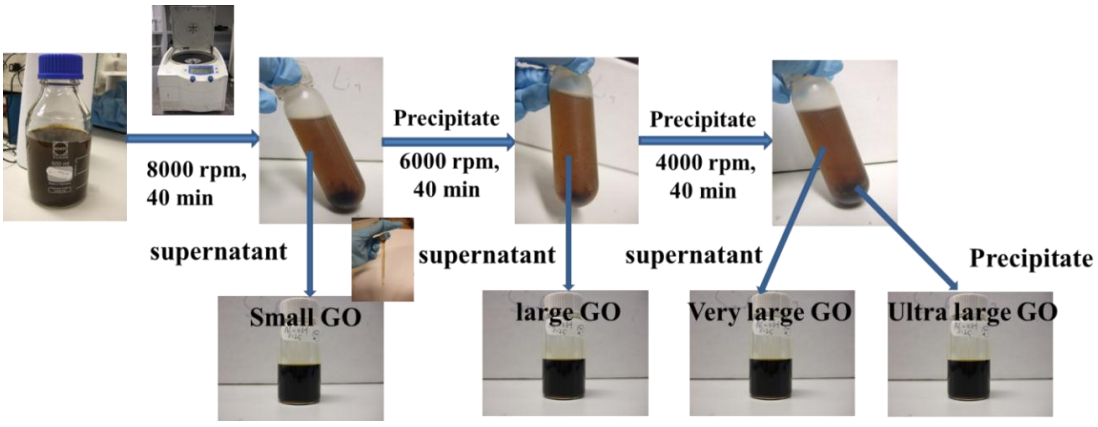

Figure 1. Flowchart for GO sorting process by 3-steps centrifugation.

2.2 Reduction

Three different methods were chosen to reduce the GO or GO papers at different stages of fabrication, as shown in Figure 2. They include i) reduction of GO sheets using hydrazine, ii) reduction of GO papers by immersing in hydrogen iodine (HI) solution and iii) reduction of GO papers through high temperature treatment. Further details of these processes are described below.

Hydrazine reduction. The GO dispersion obtained above was mixed with hydrazine (N_2H_4 in water, 35%, Aldrich) and ammonia solution ($NH_3•H_2O$, 28–30 wt. %, Wako) at a weight ratio of hydrazine to GO about 7:10. To avoid aggregation of rGO after reduction, $NH_3•H_2O$ was used to adjust the pH of rGO dispersion in the range of 9 – 11 and the temperature was controlled to maintain below 100 ℃.

Hydrogen iodine reduction. The GO papers obtained from vacuum filtration were immersed into hydroiodic acid (HI, 57%, Acros) in a sealed cuvette, and placed the cuvette in a warm oil bath for 1 hr. The reduced GO papers were washed by ethanol for three times to remove excessive HI on their surface.

Thermal reduction. The GO papers were placed inside a ceramic container which was introduced into a furnace (Thermcraft /Eurotherm) with controlled vacuum and argon flow. The papers were pre-annealed at a heating rate of 10 ℃/min, and held at 400 ℃ for 1.5 h. After cooling to room temperature, the papers were heated to 1100 ℃ and held for 30 min.

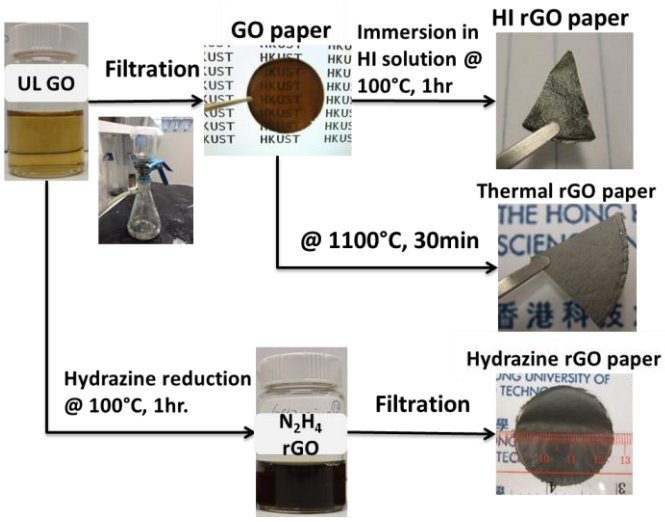

Figure 2. Flowchart for sample preparation and treatments.

2.3 Characterization and mechanical tests

The area of GO sheets as well as the thickness and surface morphology of the GO papers were examined on a scanning electron microscope (SEM, JEOL 6700F, JSM). The sorted GO dispersion was diluted using methanol in the ratio of 1:50, and its droplets were applied on the silicon wafer and dried to take clear images of GO under SEM. The SEM images of dimensions 100 μm x 130 μm were processed using the software ImageJ to analyze the areas of GO sheets. A total of more than 100 individual GO sheets were analyzed for each set of condition. The X-ray photoelectron spectroscopy (XPS, Axis Ultra DLD) was used to characterize the elemental compositions and the assignments of carbon peaks. The Raman spectroscopy (Renishaw MicroRaman/Photoluminescence System) was used to analyze the structure of GO papers using 633 nm He-Ne laser. The electrical conductivity was measured using the four probe method (Scientific Equipment & Services). The mechanical properties of

GO papers were measured on a dynamic mechanic analyzer (DMA, Perkin Elmer). 20 mm x 3 mm rectangular samples were loaded in tension with a preload of 50 mN and a controlled force ramp rate of 50 mN/min.

3 Results and discussion

3.1 GO Size distribution

Figure 3 presents typical SEM images of four different groups of sorted GO sheets and the corresponding size distributions. Their average areas were 1.0, 8.7, 32 and 264 μm^2, respectively, for the S-GO, L-GO, VL-GO and UG-GO sheets.

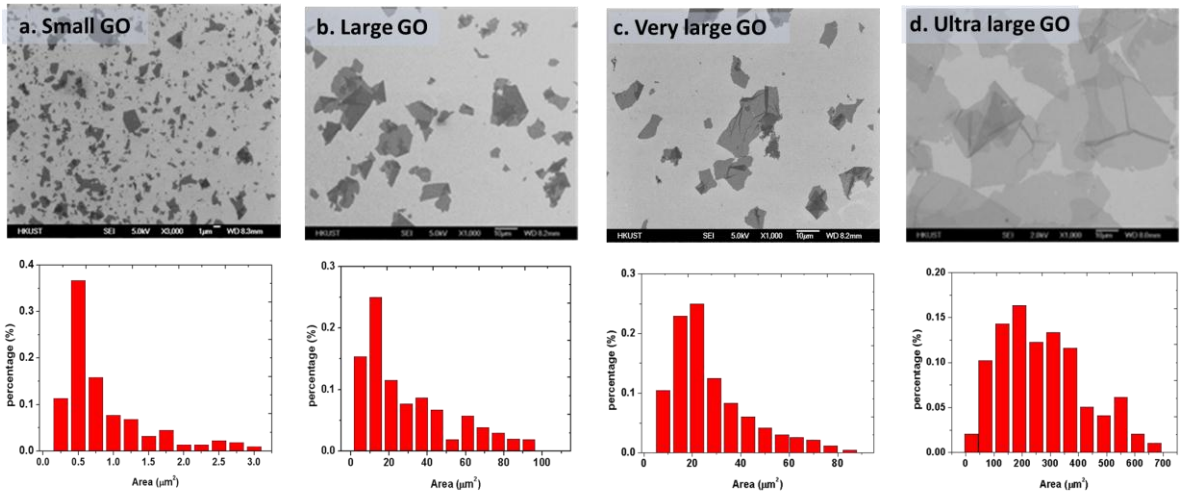

Figure 3. SEM images and the corresponding area distributions of (a) small GO, (b) large GO, (c) very large GO, and (d) ultra large GO sheets.

3.2 Surface Chemistry

The surface chemistry of GO sheets was significantly influenced by GO size. Figure 4 shows the Raman spectra of GO sheets and the corresponding I_D/I_G intensity ratio. The D band is associated with the order/disorder of the system and the G-band is an indicator of the stacking structure, and these two bands are the dominant vibrational modes for graphite structures. The intensity ratio of I_D/I_G is widely used for quantifying the defects in graphitic materials [20]. The I_D/I_G ratio systematically decreased with increasing GO size, clearly indicating a decreasing trend of defect quantity in the GO structure (Figure 4b).

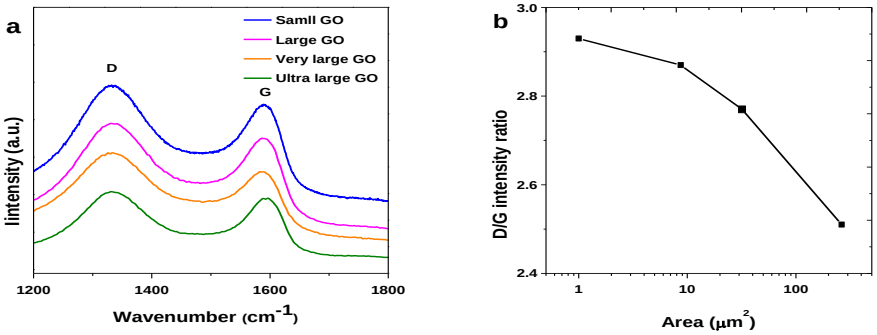

Figure 4. Raman spectra of GO sheets with four different size groups: (a) D- and G-band peaks and, (b) I_D/I_G intensity ratio as a function of average GO area.

The XPS results of GO sheets with four different size groups are presented in Figure 5 and the corresponding carbon assignations are summarized in Table 1. The binding energies of the C–C and C–H bonds are assigned at 284.7 and 285.5 eV, respectively, and the peaks at 286.7, 287.6 and 289.2 eV are assigned to -C–OH, -C=O, and -COO functional groups, respectively. The larger was the GO size the higher was the C/O ratio, suggesting that the smaller GO contained relatively more oxygenated functional groups for a given area of material. It is worth noting that the relative percentages of the carboxyl groups decreased consistently with increasing the GO size, see Table 1. According to the Lerf-Klinowski model [21], the carboxylic acids are present at the edges of the basal plane, whereas the hydroxyl and epoxide groups exist on the basal plane. As smaller GO sheets have a longer periphery length for a given area of GO sheets, the smaller GO sheets tended to contain more carboxyl groups, and vice versa for the hydroxyl and epoxide groups.

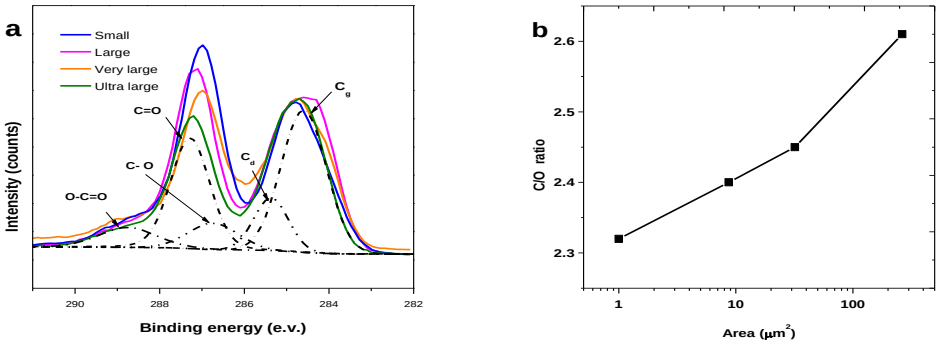

Figure 5. XPS results of GO sheets with four different size groups: (a) curve fitting of C 1s spectra, (b) C/O ratio as a function of average GO area.

Binding energy and assignation	Cg sp^2 ~284.7 eV	Cd sp^3 ~285.5 eV	C-OH ~286.7 eV	-C=O ~287.6 eV	-COO ~290.2 eV
small	38.9	12.1	9.7	28.5	10.8
large	39.6	11.4	10.3	29.7	9.0
very large	36.7	8.3	14.8	32.4	7.8
ultra large	36.8	12.7	14.4	31.0	5.1

Table 1. Relative percentages of carbon and assignations of four different size groups of GO.

3.3 Mechanical and electrical properties of GO papers

Both the Young's modulus and tensile strength of GO papers were found to increase with increasing the GO size, as shown in Figure 6. There were more than 200% increments of both properties when the average size of GO sheets was increased from 1.0 to 264 μm^2 for the same volume of materials. There are two major reasons responsible for these observations. Firstly, the papers made from larger GO sheets tended to have a more compact structure than those with smaller sheets, as proven by the X-ray diffraction analysis. The smaller GO sheets with more oxygenated functional groups could absorb more water through hydrogen bonding, which in turn led to a larger interlayer distance, inevitably increasing the cross-sectional area for a given graphene weight content. Secondly, fewer defects are present in the larger GO sheets as illustrated by the lower I_D/I_G intensity ratio.

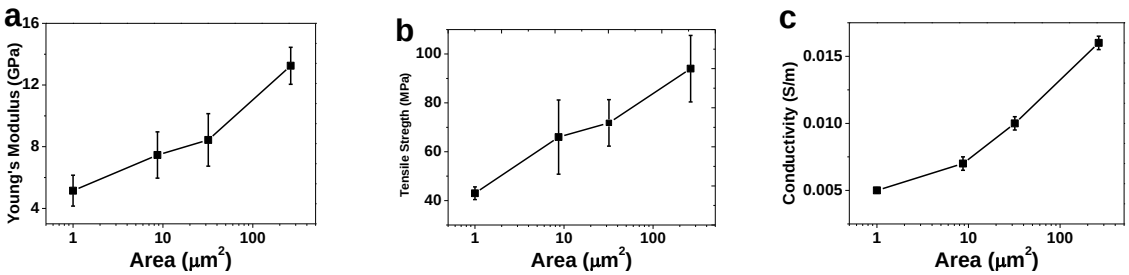

Figure 6. Changes in (a) Young's modulus, (b) tensile strength, and (c) electrical conductivity of GO papers measured before reduction as a function of average GO area.

The electrical conductivity of GO sheets before reduction increased consistently with increasing the average GO size (Figure 6c). One of the major mechanisms behind this finding is the higher inter-sheet contact resistance in the papers made from smaller GO sheets with a longer periphery length and more carboxyl groups, than in the papers containing larger sheets. The electrical conductivity of rGO papers also depended strongly on the size of their GO precursors. Figure 7 illustrates the conductivities of rGO papers reduced by three different methods, confirming the positive correlation between the GO size and the conductivity of the papers. Further discussions are made of the effects of reduction process on various properties, including the electrical conductivity, in Section 3.4.

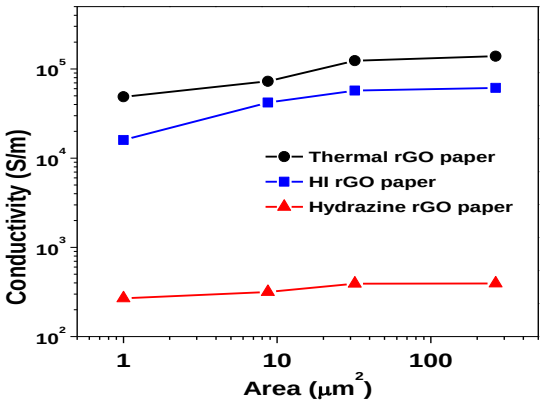

Figure 7. Conductivity of rGO papers as a function of average GO area for different reduction methods.

3.4 Effects of reduction

The XPS was used to trace the changes in elemental composition and functional groups of rGO papers after reduction. Figure 8a presents the curve fitting of the C1s peaks of XPS spectra, providing further evidence of the effects of reduction. The intensities of the sp^2 and sp^3 carbon increased, while the concentrations of –C-OH, -C=O and -COO functional groups all decreased after reduction. The chemical reduction using hydrazine or HI was proven to be effective in removing -C=O groups by ring opening of the epoxide groups [22. 23]. The thermal treatment removed the carboxyl groups (-COO) starting from around 150 ℃ and the hydroxyl groups (C-OH) at 650 ℃ [24], and after the complete thermal treatment at 1100 ℃, both the hydroxyl and carboxyl groups were almost fully eliminated. The C/O ratios were 2.6, 5.5, 7.1 16.4 for the as-produced GO, hydrazine rGO, HI rGO and thermal rGO papers, respectively. The C/O ratio is a useful measure of the degree of reduction because it represents the total carbon weight including the restored carbon conjugation with respect to the remaining oxygen weight. The high oxygen content disrupted the sp^2 bonded carbon

network, making the GO papers with the lowest C/O ratio as an insulator. The C/O ratio increased after reduction and the thermal rGO papers had the highest value of 16.4 with a single, sharp peak at 284.5 eV (Figure 8a). Figure 8b presents the electrical conductivity plotted as function of C/O ratio. The effective removal of functional groups restored the sp^2 carbon, improving the electrical conductivity. The thermal reduction exhibited the highest conductivity corresponding to the highest degree of reduction.

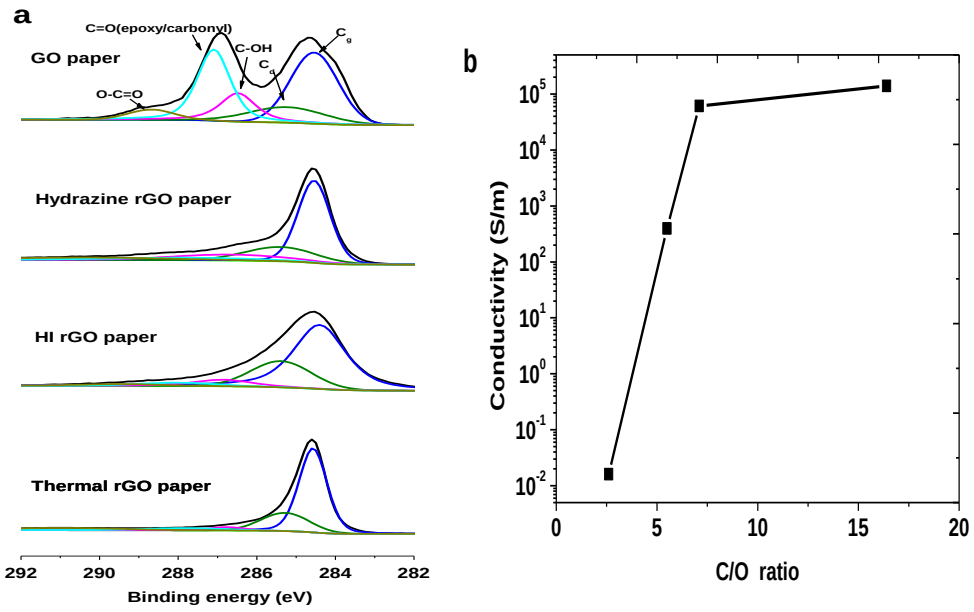

Figure 8. XPS results of as-produced GO and rGO papers: (a) curve fitting of C 1s spectra, (b) electrical conductivity of UL-rGO papers as a function of C/O ratio.

4 Conclusions

Using simple and effective centrifugation-based sorting process, UL-GO sheets were fabricated with an average size of 264 μm^2. The GO papers made from larger GO sheets demonstrated higher mechanical and electrical properties than those made from smaller size GO. The rGO papers reduced by thermal treatment presented the highest conductivity of 139,000 S/m among three different reduction methods studied. The development of UL-GO sheets and effective thermal treatment methods could open a new avenue for mass production of high-quality GO precursor with controlled size and excellent inherent properties.

References

[1] Park S., Lee K., Bozoklu G., Cai W., Nguyen S.B.T., Ruoff R.S. Graphene oxide papers modified by divalent ions - Enhancing mechanical properties via chemical cross-linking. *ACS Nano*, **2**, pp. 572-578 (2008).

[2] Dikin D.A., Stankovich S., Zimney E.J., Piner R.D., Dommett G.H.B., Evmenenko G., Nguyen S.T., Ruoff R.S. Preparation and characterization of graphene oxide paper. *Nature*, **448**, pp. 457-460 (2007).

[3] Ranjbartoreh A.R., Wang B., Shen X., Wang G. Advanced mechanical properties of graphene paper. *J. Appl. Phys.*, **109** (2011).

[4] Barnard A.S., Snook I.K. Thermal stability of graphene edge structure and graphene nanoflakes. *J. Chem. Phys.*, **128** (2008).

[5] Compton O.C., Dikin D.A., Putz K.W., Brinson L.C., Nguyen S.T. Electrically Conductive "Alkylated" Graphene Paper via Chemical Reduction of Amine-Functionalized Graphene Oxide Paper. *Adv Mater*, **22**, pp. 892-896 (2010).

[6] Chen H., Müller M.B., Gilmore K.J., Wallace G.G., Li D. Mechanically strong, electrically conductive, and biocompatible graphene paper. *Adv Mater,* **20**, pp. 3557-3561 (2008).
[7] Huang Z.D., Zhang B., Zheng Q.B., Oh S.W., Lin X.Y., Yousefi N., Kim J.K. Self-assembled graphene oxide/carbon nanotube films as electrodes for supercapacitors. *J. Mater. Chem.,* **22**, pp. 3591-3599 (2011).
[8] Hu W., Peng C., Luo W., Lv M., Li X., Li D., Huang Q, Fan C. Graphene-Based Antibacterial Paper. *ACS Nano,* **4**, pp. 4317-4323 (2010).
[9] Xu Y., Sheng K., Li C., Shi G. Self-assembled graphene hydrogel via a one-step hydrothermal process. *ACS Nano,* **4**, pp. 4324-4330 (2010).
[10] Becerril H.A., Mao J., Liu Z., Stoltenberg R.M., Bao Z., Chen Y. Evaluation of solution-processed reduced graphene oxide films as transparent conductors. *ACS Nano,* **2**, pp. 463-470 (2008).
[11] Yousefi N., Gudarzi M.M., Zheng Q.B.**,** Aboutalebi S. H., Sharif F. and Kim J.K. Self-alignment and high electrical conductivity of ultralarge graphene oxide/polyurethane nanocomposites. *J. Mater. Chem.,* DOI:10.1039/C2JM30590A.
[12] Zheng Q.B., Ip W.H., Lin X.Y., Yousefi N., Yeung K.K., Li Z.G., Kim J.K. Transparent conductive films consisting of ultralarge graphene sheets produced by Langmuir-Blodgett assembly. *ACS Nano,* **5**, pp. 6039-6051 (2011).
[13] Balandin A.A., Nika D.L., Ghosh S., Pokatilov E.P. Lattice thermal conductivity of graphene flakes: Comparison with bulk graphite. *Appl. Phys. Lett.,* **94** (2009).
[14] Peng X., Liu X., Diamond D., Lau K.T. Synthesis of electrochemically-reduced graphene oxide film with controllable size and thickness and its use in supercapacitor. *Carbon,* **49**, pp. 3488-3496 (2011).
[15] Kim K.S., Zhao Y., Jang H., Lee S.Y., Kim J.M., Kim K.S., Ahn J., Kim P., Choi J., Hong B.H. Large-scale pattern growth of graphene films for stretchable transparent electrodes. *Nature,* **457**, pp. 706-710 (2009).
[16] Pan S., Aksay I.A. Factors controlling the size of graphene oxide sheets produced via the graphite oxide route. *ACS Nano,* **5**, pp. 4073-4083 (2011).
[17] Wang X., Bai H., Shi G., Size fractionation of graphene oxide sheets by pH-assisted selective sedimentation. *J. Am. Chem. Soc.,* **133**, pp. 6338-6342 (2011).
[18] Geng Y., Wang S.J., Kim J.K., Preparation of graphite nanoplatelets and graphene sheets. *J. Colloid Interf. Sci.,* **336**, pp. 592-598 (2009).
[19] Aboutalebi S.H., Gudarzi M.M., Zheng Q.B., Kim J.K. Spontaneous formation of liquid crystal in ultralarge graphene oxide dispersions. *Adv. Funct. Mater.,* **21**, pp. 2978–2988 (2011).
[20] Pimenta M.A., Dresselhaus G., Dresselhaus M.S., Cançado L.G., Jorio A., Saito R. Studying disorder in graphite-based systems by Raman spectroscopy. *Phys. Chem. Chem. Phys.,* **9**, pp. 1276-1291 (2007).
[21] Casabianca L.B., Shaibat M.A., Cai W.W., Park S., Piner R., Ruoff R.S., Ishii Y. NMR-based structural modeling of graphite oxide using multidimensional 13C solid-state NMR and ab initio chemical shift calculations. *J. Am. Chem. Soc.,* **132**, pp. 5672-5676 (2010).
[22] Dreyer D.R., Park S.J., Bielawski C.W., Ruoff R.S. The chemistry of graphene oxide. Chem. Soc. Rev., **39**, 228–240 (2010).
[23] Wang S.J., Geng Y., Zheng Q.B., Kim J.K. Fabrication of highly conducting and transparent graphene films. *Carbon,* **48**, pp. 1815-1823 (2010).
[24] Gao X., Jang J., Nagase S. Hydrazine and thermal reduction of graphene oxide: Reaction mechanisms, product structures, and reaction design. *J. Phys. Chem. C,* **114**, pp. 832-842 (2010).